Biochimica et Biophysica Acta 1843 (2014) 2991–3003

Contents lists available at ScienceDirect

Biochimica et Biophysica Acta

journal homepage: www.elsevier.com/locate/bbamcr

Physiologically induced restructuring of focal adhesions causes mobilization of vinculin by a vesicular endocytic recycling pathway

María Gabriela Márquez [a,b], Yamila Romina Brandán [a,b], Edith del Valle Guaytima [a,b], Carlos Humberto Paván [b], Nicolás Octavio Favale [b,c], Norma B. Sterin-Speziale [b,*]

[a] Instituto de Investigaciones en Ciencias de la Salud Humana (IICSHUM), Universidad Nacional de La Rioja, Av. Luis Vernet 1000, 5300 La Rioja, Argentina
[b] Instituto de Química y Físico-Química Biológica (IQUIFIB)-CONICET, Facultad de Farmacia y Bioquímica, Universidad de Buenos Aires, Junín 956, C1113AAD Buenos Aires, Argentina
[c] Cátedra de Biología Celular, Departamento de Ciencias Biológicas, Facultad de Farmacia y Bioquímica, Universidad de Buenos Aires, Junín 956, C1113AAD Buenos Aires, Argentina

ARTICLE INFO

Article history:
Received 18 December 2013
Received in revised form 11 September 2014
Accepted 13 September 2014
Available online 18 September 2014

Keywords:
Vinculin
Cytosolic pool
Focal adhesion
Bradykinin
Vesicle recycling

ABSTRACT

In epithelial cells, vinculin is enriched in cell adhesion structures but is in equilibrium with a large cytosolic pool. It is accepted that when cells adhere to the extracellular matrix, a part of the soluble cytosolic pool of vinculin is recruited to specialized sites on the plasma membrane called focal adhesions (FAs) by binding to plasma membrane phosphatidylinositol-4,5-bisphosphate (PtdIns(4,5)P_2). We have previously shown that bradykinin (BK) induces both a reversible dissipation of vinculin from FAs, by the phospholipase C (PLC)-mediated hydrolysis of PtdIns(4,5)P_2, and the concomitant internalization of vinculin. Here, by using an immunomagnetic method, we isolated vinculin-containing vesicles induced by BK stimulation. By analyzing the presence of proteins involved in vesicle traffic, we suggest that vinculin can be delivered in the site of FA reassembly by a vesicular endocytic recycling pathway. We also observed the formation of vesicle-like structures containing vinculin in the cytosol of cells treated with lipid membrane-affecting agents, which caused dissipation of FAs due to their deleterious effect on membrane microdomains where FAs are inserted. However, these vesicles did not contain markers of the recycling endosomal compartment. Vinculin localization in vesicles has not been reported before, and this finding challenges the prevailing model of vinculin distribution in the cytosol. We conclude that the endocytic recycling pathway of vinculin could represent a physiological mechanism to reuse the internalized vinculin to reassembly new FAs, which occurs after long time of BK stimulation, but not after treatment with membrane-affecting agents.

1. Introduction

Vinculin is an important constituent of both adhesion junctions and focal adhesions (FAs), and is expressed in most cell types and tissues [1,2]. FAs are membrane multi-protein complexes involved in cell attachment to the extracellular matrix, where actin stress fibers and the extracellular matrix (ECM) are connected [3]. It is accepted that intracellular vinculin exists either as a soluble cytosolic pool or as a cytoskeleton-bound pool [4]. When cells adhere and spread on the ECM, a part of the cytosolic vinculin is recruited to FAs. In fibroblasts, it has been reported that vinculin's half-life is 2–3 times shorter in the cytoskeletal than in the cytosolic pool [4]. In the cytosol, vinculin adopts an auto-inhibited conformation by an intramolecular interaction between its globular N-terminal head (Vh) and the carboxy-terminal tail (Vt), masking the numerous partner-binding sites in the protein by steric and allosteric mechanisms [5–7]. Biochemical and structural studies have established that the acidic phospholipid phosphatidylinositol-4,5-bisphosphate (PtdIns(4,5)P_2) can disrupt the interaction between Vh and Vt by binding to the Vt domain [8], exposing binding sites for talin, α-actinin, α-catenin, VASP, vinexin, ponsin, Arp2/3, paxillin, and actin [9]. Alternatively, some authors have proposed a combinatorial pathway requiring at least two binding partners at sites of cell adhesion [10], and others have suggested that vinculin can also be activated by a single ligand such as talin or α-actinin [11]. FAs have been associated with detergent-resistant microdomains (DRM) as well as with local membrane accumulation of PtdIns(4,5)P_2 [12]. In rat renal papillary collecting duct cells, we have shown that FAs are part of DRM that are highly enriched in cholesterol and polyphosphoinositides, whose lipid composition corresponds to the physiological environment where FAs are inserted [13].

We have previously demonstrated that the endogenous intrarenal hormone bradykinin (BK) induces a transient restructuring of FAs in renal papillary collecting duct cells, by a reversible dissociation of vinculin (but not of talin) from FAs, thus evoking the reorganization of the actin cytoskeleton, preserving cell attachment to the ECM, and maintaining cell-to-cell connections [14]. We further reported that BK-induced vinculin-stained FA dissipation occurs concomitantly with a non-pinocytic, non-caveolar-mediated vinculin internalization and

* Corresponding author at: Departamento de Ciencias Biológicas, Facultad de Farmacia y Bioquímica, Universidad de Buenos Aires, Junín 956, C1113AAD Buenos Aires, Argentina. Tel.: +54 11 49648238; fax: +54 11 49625457.
E-mail address: speziale@ffyb.uba.ar (N.B. Sterin-Speziale).

http://dx.doi.org/10.1016/j.bbamcr.2014.09.014
0167-4889/

that part of the internalized vinculin colocalizes with the transferrin receptor (TfR) [15]. In this work, we isolated vinculin-containing vesicles to characterize them morphologically and biochemically. We further studied the properties of the association of vinculin with intracellular vesicles, and, by analyzing the proteins involved in vesicle traffic, we propose a model for intracellular vesicle traffic of vinculin.

2. Materials and methods

2.1. Antibodies and reagents

Monoclonal vinculin, talin, paxillin and cyclin D antibodies were purchased from Sigma-Aldrich. The polyclonal antibodies against Rab5, Rab11, and CD71 (transferrin receptor), and the monoclonal Na, K-ATPase β_1 were from Santa Cruz Biotechnology, Inc. The biotinylated anti-PtdIns(4,5)P_2 was from Echelon Biosciences, Inc. Goat anti-rabbit or goat anti-mouse secondary antibodies conjugated to either TRITC or FITC, and affinity purified rabbit anti-mouse IgG (Fc) were from Jackson ImmunoResearch Inc. Enhanced chemiluminescence (ECL) kit was from GE Healthcare Life Sciences, and avidin–biotin–peroxidase kit was from Dako Lab. All culture reagents were from Gibco, Invitrogen. Magnetic beads (Dynabeads M-500 Subcellular) and magnetic device were from Dynal, Invitrogen. All other reagents and chemicals, unless otherwise stated, were from Sigma-Aldrich, or Merck, and purchased from local commercial suppliers.

2.2. Animals and tissue preparation

Male Wistar rats (250–300 g) were housed in a light-controlled room with a 12:12 h light-dark cycle and allowed free access to water and standard rat chow. All animals were handled according to the rules for animal care and use of laboratory animals of the University of Buenos Aires. The animal protocol was reviewed and approved by the Ethics Committee for the care and use of laboratory animals, School of Pharmacy and Biochemistry, University of Buenos Aires (CICUAL-FFYB). Animals were killed by decapitation, kidneys removed and renal papillae isolated and collected in ice-cold 10 mM Tris–HCl, pH 7.4, containing 140 mM NaCl, 5 mM KCl, 2 mM $MgSO_4$, 1 mM $CaCl_2$ and 5.5 mM glucose (TSS). Renal papillae were sliced (0.5 mm thick) by using a Stadie–Riggs microtome and collected in ice-cold TSS, and incubated at 37 °C in a metabolic shaking bath either in the absence or in the presence of 1 μM BK for 5 min, 1 mM neomycin for 10 min or 5 mM methyl-β-cyclodextrin for 30 min. Incubations were stopped on ice and immediately homogenized in 10 vol of a solution 0.25 M sucrose containing 25 mM Tris–HCl, pH 7.4, 3 mM $MgCl_2$, 2 mM EGTA, 1 mM PMSF, 10 μg/ml aprotinin and 1 mM Na_3VO_4. The resulting homogenate was centrifuged at 860 *g* for 10 min. The postnuclear supernatants were pooled and centrifuged at 105,000 *g* for 60 min. The resulting pellet and supernatant were used as microsomal and cytosolic fractions. Depending on the experiment, the postnuclear supernatant or microsomes were used as starting material for vesicle immunoisolation. Aliquots from the resulting postnuclear supernatants, microsomal and cytosolic fractions were assayed for protein content by the method of Lowry. To study the purity of the subcellular fractions we determined the presence of Na, K-ATPase in microsomal and cytosolic fractions by Western blot analysis.

2.3. Immunoisolation of vinculin-containing vesicles

Vesicles were immunoisolated by applying the protocol provided by the manufacturer. In the direct technique, the postnuclear supernatant or the microsomal fraction was incubated for 12 h at 4 °C on a rotation wheel with magnetic beads coated with 8 μg of vinculin monoclonal antibody/10^7 beads in PBS pH 7.4 containing 2 mM EDTA and 5% fetal calf serum (buffer A), in a relation of 200 μg of unpurified subcellular fraction per 1.4×10^7 beads. In the indirect technique, the unpurified cellular fraction was previously incubated with saturating amounts of anti-vinculin antibody, and after removing the unbound antibody by ultracentrifugation, we performed the incubation with the beads coated with the linker antibody following the procedure described in the direct technique. To perform the immunoisolation of vesicles, we added 700 μl of Dynabeads (containing 1.4×10^7 beads) to 300 μl of postnuclear supernatant or microsomal fraction (containing 200 μg of protein), and at the end of the incubation, the tube was placed in a magnet for 2–3 min, the beads with the attached vesicles were washed with buffer A (3×15 min), and resuspended in 70–100 μl of the same buffer. As a negative control, we used beads where vinculin antibody was omitted or beads coated with anti-cyclin D monoclonal antibody as an irrelevant antibody. When the postnuclear supernatant was used as starting material, the nonbound subfraction (~1 ml) was saved for analysis. In this way, the starting material was resolved in two subfractions: "nonbound" and "bound", respectively. Aliquots from the two subfractions were assayed for protein content by the method of Lowry. Volumes of the nonbound and bound subfractions were adjusted to contain the same amount of total protein for immunoblot analysis.

2.4. Electron microscopy

Electron microscopy was performed to visualize the elements immunoisolated on the magnetic beads. The bound subfraction, and the beads whose the primary antibody had been omitted, were fixed in a mixture of 4% formaldehyde, 1.5% glutaraldehyde and 0.1 M cacodylate buffer pH 7.3 at room temperature for 2 h, then washed and postfixed in 1% osmium tetroxide. Afterward, the material was dehydrated in acetone and embedded in Araldite (Electron Microscopy Sciences, Hatfield, PA, USA). Thin sections were cut in a JEOL ultramicrotome with a diamond knife. The ultrathin sections were contrasted with uranyl acetate and lead citrate. Observations were made using a LEO 906-E transmission electron microscope (Carl Zeiss) and photographed with a megaview III camera.

2.5. Mass spectroscopy

The LC–MS/MS analysis was performed in the Laboratorio Nacional de Investigación y Servicios en Péptidos y Proteínas y Espectrometría de Masa (Lanais Pro Em-Conicet — Argentina). A homogenate of BK-treated renal papillae was centrifuged at 4000 *g* for 10 min at 4 °C. The pellet was resuspended in 1 ml of a solution 0.25 M sucrose containing 25 mM Tris–HCl, pH 7.4, 3 mM $MgCl_2$, 2 mM EGTA, 1 mM PMSF, 10 μg/ml aprotinin and 1 mM Na_3VO_4 and then recentrifuged under the same conditions. The pellets were discarded, and the supernatant was centrifuged at 17,000 *g* for 20 min at 4 °C. The pellet obtained represents the high density (HD) membrane fraction. The supernatant was collected and centrifuged at 200,000 *g* for 60 min at 4 °C. The pellet was resuspended in 500 μl of PBS and was centrifuged for another 60 min under the same conditions. The resulting pellet was resuspended in 520 μl of PBS. This low density (LD) membrane suspension was used for immunoisolation of vinculin-containing vesicles. LD membranes (200,000 *g* pellet, 1000 μg of protein) were added to 400 μl of magnetic beads coated with 8 μg of vinculin monoclonal antibody/10^7 beads and mixed for 17 h at 4 °C. The supernatant was then discarded, and the beads were then washed with PBS pH 7.4 containing 2 mM EDTA (3×15 min), and resuspended in 400 μl of the same buffer. An aliquot of 350 μl of the immunoisolated vesicles from LD membranes was used to perform the mass spectroscopy analysis and the rest to investigate the presence of vinculin by immunoblot. Proteins were eluted and solubilized by addition of Laemmli sample buffer followed by heating to 100 °C for 5 min. The 200,000 *g* pellet from this procedure is virtually devoid of plasma membranes based on immunoblotting with antibodies to plasma membrane marker proteins [16,17]. To verify this conclusion, we determined the presence of Na, K-ATPase in HD and LD fractions by Western blot analysis. Immunoisolated vinculin vesicle

proteins were separated by SDS-PAGE using 10% polyacrylamide minigels. Gels were then stained for 40 min with Coomassie blue to visualize the proteins. The color bands (≥40 kDa molecular weight) were cut and then destained with methanol:water:acetic acid (50:50:1) for 120 min at room temperature until entirely destained. Gel samples were dried and then reduced with 10 mM DTT in 100 mM NH_4HCO_3, for 1 h at 56 °C. The supernatant was removed and an aqueous solution containing 55 mM iodacetamide in 100 mM NH_4HCO_3 was added for 45 min in darkness at 22 °C to alkylate the reduced cysteine residues. The supernatant was then removed, and gels were washed twice with acetonitrile with 100 mM NH_4HCO_3 for 15 min. Proteins were trypsinized using 25 ng/μl sequencing grade modified trypsin (Promega, Madison, WI), diluted in 50 mM NH_4HCO_3 and incubated at 37 °C for 16 h. Peptides were extracted from the gel in 50% acetonitrile, 0.5% formic acid solution, then dried, and reconstituted with 0.1% formic acid.

Tryptic peptides from each gel block were analyzed by one-dimensional LC–MS/MS using LCQ Duo (Thermo Finnigan, San José, CA). Chromatographic separation of peptides was accomplished using reverse phase C_{18} column 250 × 1.0 mm (Vydac 218TP51). The gradient was 2–15% solvent B (80% acetonitrile, 0.1% formic acid) in solvent A (0.1% formic acid) in 10 min, 15–50% solvent B in solvent A in 70 min, 50–80 % solvent B in solvent A in 8 min, 80–100% solvent B in solvent A in 2 min, and 100% solvent B in 2 min at a flow rate of about 100 μl/min.

The *m/z* ratios of peptides and their fragmented ions were recorded by a method that allows the acquisition of three MS^2 scans (i.e. for the three highest intensity peaks in MS^1 scans) following each full MS scan. The raw data files were searched against the global protein data base from SwissProt and using BioWorks (Version 3) software (Thermo Finnigan) bases on the Sequest algorithm and Mascot Search engine. The search parameters included the following: precursor ion mass accuracy = 1.7 amu, fragment ion mass accuracy = 0.6 amu, modification allowed for carboxyamidomethylation, and two missed cleavages allowed. After the peptide sequence and protein identification from BioWorks software was carried out, the identified peptide sequences were initially quantified and filtered using the cross correlation score (Xcorr) at the following threshold: Xcorr > 1.5 for 1 + ion, 2.0 for 2 + ion, and 2.5 for 3 + ion. A list of proteins (≥40 kDa) whose identifications were validated by identification of two or more component peptides or one peptide and manual inspection of spectrum is given.

2.6. Immunoblot analysis

Renal papilla postnuclear supernatant, microsomal and cytosolic fractions, as well as HD and LD membrane fractions, and bead-bound vesicles were resolved by electrophoresis in a 10% SDS-polyacrylamide gel under reducing conditions, and transferred to polyvinylidene difluoride (PVDF) membranes. After blotting, membranes were treated with 5–10% nonfat milk in TBS-Tween 20 and incubated with the indicated antibodies. Primary interaction was evidenced by using the enhanced chemiluminescence kit (ECL), or avidin–biotin–peroxidase and 3,3′diaminobenzidine. For loading control, lines corresponding to the IgG heavy chain (~55 kDa) are shown. The blots were scanned and signals quantified by optical densitometry with a Gel-Pro Analyzer 3.1. For reprobing, the blots were stripped in a buffer containing 100 mM 2-mercaptoethanol, 2% sodium dodecyl sulphate, and 62.5 mM Tris–HCl.

2.7. Membrane extraction

For high-salt and alkaline extraction, the microsomal fractions prepared from the renal papilla slices treated with 1 μM BK for 5 min (150–200 μg protein) were adjusted to 0.1 M Na_2CO_3, 0.5 M Na_2CO_3, 1 M KCl, 2 KClM, and 3 M KCl by the addition of respective stock solutions of 1 M Na_2CO_3 pH 10 or 3 M KCl made in 10 mM Tris/HCl pH 7.4, and incubated at room temperature for 30 min. To pellet the insoluble fraction, the suspensions were centrifuged at 100,000 *g* for 1 h. The pellets were solubilized in SDS sample buffer, and the supernatants were precipitated in trichloroacetic acid and solubilized in SDS sample buffer. The pellets and supernatant fractions were adjusted to equal volumes and analyzed for vinculin by immunoblot analysis.

2.8. Triton X-114 phase separation

The microsomal fraction prepared from the renal papilla slices treated with 1 μM BK for 5 min (200 μg protein) was resuspended in 200 μl of 1% Triton X-114, 10 mM Tris/HCl pH 7.4, and 150 mM NaCl, followed by the phase separation by incubation for 10 min at 4 °C, and then transferred to 30 °C for 20 min. The samples were briefly spun in a microcentrifuge to separate the lower detergent-rich phase from the upper aqueous phase, and both phases were dissociated and the presence of vinculin or transferrin receptor in each phase was analyzed by immunoblot. Integral proteins partition into the detergent phase, whereas most peripheral proteins go into the aqueous phase [18].

2.9. Protease protection assay

Freshly prepared microsomal fractions from renal papilla slices treated with BK (100 μg protein in 320 mM sucrose and 10 mM HEPES pH 7.4) were adjusted to 10 mM $CaCl_2$ and incubated at 0 °C for 40 min with 10 μg and 40 μg of trypsin, with or without 1% Triton X-100. After 30 min, 40 μg of aprotinin was added to each sample, and incubation was continued for 5 min on ice. After ultracentrifugation (100,000 *g* for 1 h) the protease-resistant membrane fraction recovered in pellets was analyzed for vinculin and Na,K-ATPase β subunit by immunoblot analysis.

2.10. Cell cultures

Primary cultures of papillary collecting duct cells were performed according to Stokes et al. [19]. Briefly, renal papillae were minced to 1–2 mm^3 pieces and incubated at 37 °C in sterile TBS containing 0.1% collagenase II under 95%O_2/5%CO_2. After 40 min, digestion was stopped and isolated cells and structures were separated by centrifugation at 175 *g* for 10 min. The crude pellet containing most papillary cell types, tubular structures and tissue debris was washed twice and resuspended in Dulbecco's modified Eagle's medium (DMEM) with F-12 (1:1), 10% fetal bovine serum (Natocor, Córdoba, Argentina), 100 U/ml penicillin and 100 μg/ml streptomycin. The enriched collecting duct pellets were obtained by centrifugation at 60 g for 1 min and resuspended in an adequate volume of DMEM/F12. Enriched-tubular suspensions were seeded in sterile dry-glass coverslips placed in six-well multidishes. After growing at 37 °C for 96 h, cultures were treated with 1 μM BK for 1, 5 and 10 min, 5 mM methyl-β-cyclodextrin for 30 min, or 1 mM neomycin for 10 min. Incubations were stopped on ice and cells rapidly processed for microscopy.

2.11. Cell labeling and immunofluorescent microscopy

For immunostaining, cells treated as described above were fixed with methanol (at −20 °C for 10 min) and acetone (at −20 °C for 4 min), and blocked with 3% goat normal serum in PBS. After fixation, cells were incubated with the appropriate combinations of antibodies overnight at 4 °C in goat serum containing PBS. Mouse and rabbit primary antibodies were detected using fluorescent FITC or TRITC conjugated goat anti-mouse or anti-rabbit. Finally, the cells were mounted using Vectashield Mounting Media (Vector Laboratories) and stored at 4 °C until analysis. Specimens were examined with an Olympus FV300 Confocal Microscope (Model BX61), with an acquisition software FluoView version 3.3 provided by the manufacturer. Double fluorescence for green and red channels was visualized by using an argon–helium–neon laser. Double-stained confocal images were obtained by sequential

scanning for each channel to eliminate the crosstalk of chromophores and to ensure the reliable quantification of colocalization. Confocal images represent a single Z section. All images were obtained with a cooled CCD camera and processed for output purposes using Adobe Photoshop software. We applied a "gauss filter" to soften the images with the Image-Pro Plus Version 5.1.2 (Media Cybernetics, USA) module.

2.12. Quantitative colocalization analysis

The confocal images were analyzed using the Image-Pro Plus version 5.1.2 (Media Cybernetics, USA). Six-ten randomly selected cells were analyzed for generation of quantitative data set for each treatment, and three independent experiments were performed. Cells were examined with a 100× Plan Apo oil objective (NA 1.4). Confocal horizontal optical cross sections from the medial cellular region were collected. Colocalization of antigens was evaluated quantitatively by the colocalization command of the Image-Pro Plus version 5.1.2. The Manders' Overlap Coefficient (MOC) was used to estimate the degree of colocalization [20]. Its value is defined from 0 to 1, and a MOC $\geq$ 0.7 indicates colocalization and implies that 70% of both its components overlap with the other part of the image. Two additional overlap coefficients, K1 and K2, were also calculated. These coefficients split the value of colocalization into two separate parameters, thus allowing the determination of the contribution of each antigen to the areas with colocalization. Calculations were performed in the perinuclear and marginal regions of the cells serving as a region of interest. To this end, the contour of the perinuclear and marginal regions of the cells in the confocal image (area of interest) was manually drawn by using the mouse pointer of the program. The images were "segmented" with the segmentation software command. This application segments the image into colocalizing objects (white) and background (black).

2.13. Statistical analysis

Results are expressed as means ± SEM. Data from control and different treatments were analyzed by ANOVA and significant differences were assessed by the unpaired t-test, or by one sample t test with a hypothetical mean of 100. Statistical significance was set at $p < 0.05$.

3. Results

3.1. Isolation and characterization of vinculin-containing vesicles

In previous works performed with primary cultures of rat renal papillary collecting duct cells, immunofluorescence microscopy allowed us to observe that, after short times of BK stimulation, most of the vinculin from FAs disappears and concomitantly accumulates in the perinucleus, and that, after 10 min, perinuclear accumulation dissipates and vinculin-stained FAs reassemble [13,14]. In the present work, the appearance of BK-induced internalized vinculin seems to be vesicularly associated (Fig. 1A). To corroborate the existence of vinculin-containing vesicles, we first attempted to isolate them using an immunoisolation purification protocol with an anti-vinculin monoclonal antibody on magnetic beads, coated with anti-mouse antibodies. As starting material, we used either the microsomal fraction or the postnuclear supernatant obtained from renal papillary slices stimulated with BK for 5 min. We also analyzed the presence of vinculin in total microsomes and in the cytosolic fractions. The presence of Na,K-ATPase was used as a microsome-specific marker to validate separation of fractions. Vinculin was found in both the microsomal and cytosolic fractions, while Na,K-ATPase was almost undetectable in the cytosolic fraction (Fig. 1B).

We tested two available protocols to isolate vinculin-containing vesicles: the direct technique for exposed epitopes and the indirect technique for both exposed and buried epitopes. Bead-bound vesicles were then recovered with a magnet. To verify the isolation of vinculin-containing vesicles, we analyzed the presence of vinculin by immunoblot. In both protocols, we obtained positive signal in the immunoblot, suggesting that vinculin is exposed on the surface of the vesicles (Fig. 1C). Thereafter, due to its speed and efficiency of isolation, we decided to use the direct technique for further analysis. To perform the immunoisolation of vesicles by the direct technique, we added 700 μl of beads (1.4×10^7 beads) to 300 μl of postnuclear supernatant used as started material (containing 200 μg of protein), and after incubation the tube was placed in the magnet. The target vesicles (bound fraction, B) remained bound to the beads, and the supernatant (~1 ml) – which corresponds to our nonbound fraction (NB) – was collected. Aliquots of both subfractions were analyzed. As expected, vinculin was found not only in the postnuclear supernatant and in the bound fraction, but also in the not-bound fraction (Fig. 1D). The high signal observed in the immunoblot corresponding to the bound fraction was due to the large amount of starting material used for the immunoisolation. About the origin and status of nonbound fraction of vinculin, when the postnuclear supernatant was used as started material, vinculin present in NB fraction probably corresponds to the large preexisting cytosolic pool observed in Fig. 1A, and the newly synthesized, presumably reflecting vinculin with buried epitope. In our interpretation, the majority of the nonbound fraction of vinculin corresponds to the soluble cytosolic pool, and in a much smaller proportion membrane bound vinculin present in the microsomes. We have previously demonstrated that the membrane bound vinculin is part of detergent resistant microdomain (rafts) that exists at much smaller concentration than the soluble cytosolic pool [13]. The bound fraction is expected to correspond only to the vinculin mobilized by BK treatment. As a negative control, we used beads coated with anti-cyclin D mAb as an irrelevant antibody. No vinculin was found in these beads (Fig. 1E). Thereafter, the bound subfraction was morphologically analyzed by electron microscopy. In the control sample, in which the primary antibody had been omitted, no bound material was observed (Fig. 1Fa), while in the immunoadsorbed sample, small vesicles free of content were observed (Fig. 1Fb and c).

To better characterize the bead-bound vesicles, we carried out a differential centrifugation to obtain sufficient quantity of purified material to be analyzed by mass spectrometry (Fig. 2A). Vesicles containing vinculin were immunoisolated from the LD membrane fraction of BK-treated renal papilla slices, and the associated proteins were separated by SDS-PAGE. Color bands (≥40 kDa molecular weight) were sliced into blocks, and then each block was subjected to in-gel trypsinization and elution of the resulting peptides. To confirm the specificity of the vinculin vesicle immunoisolation, aliquots containing 40 μg of protein of the 4000 *g* for 10 min centrifugation supernatant (SN), HD and LD membrane fractions, and bead-bound vesicles (~50 μl) were analyzed by Western blot. As expected, vinculin was found not only in the bound fraction but also in SN, HD and LD membrane fraction samples but with a different intensity (Fig. 2B). The signal present in HD fraction may correspond to the membrane bound vinculin present in the microsomes, and the band present in LD membrane fraction to the vesicle bound form.

Following trypsinization and extraction from each gel slice (Fig. 2C), the peptides were analyzed by LC–MS/MS. The associated proteins were identified by comparison with the rat protein data SwissProt using BioWorks Version 3.1 software. A list of proteins (≥40 kDa) whose identifications were validated by identification of two or more component peptides or one peptide and manual inspection of spectrum is shown in Table 1. We identified proteins belonging to the trafficking and cytoskeletal/motor protein categories such as actin and several actin-related proteins (alpha-actinin-4), actin-based motor proteins (myosin-9), and microtubule proteins. The immunoisolated vinculin vesicles also contained many endoplasmic reticulum-resident proteins consistent with the presence of vinculin in the rough endoplasmic reticulum. Furthermore there were several mitochondrial (ATP synthase subunit alpha and beta), and unclassified proteins (heat shock proteins,

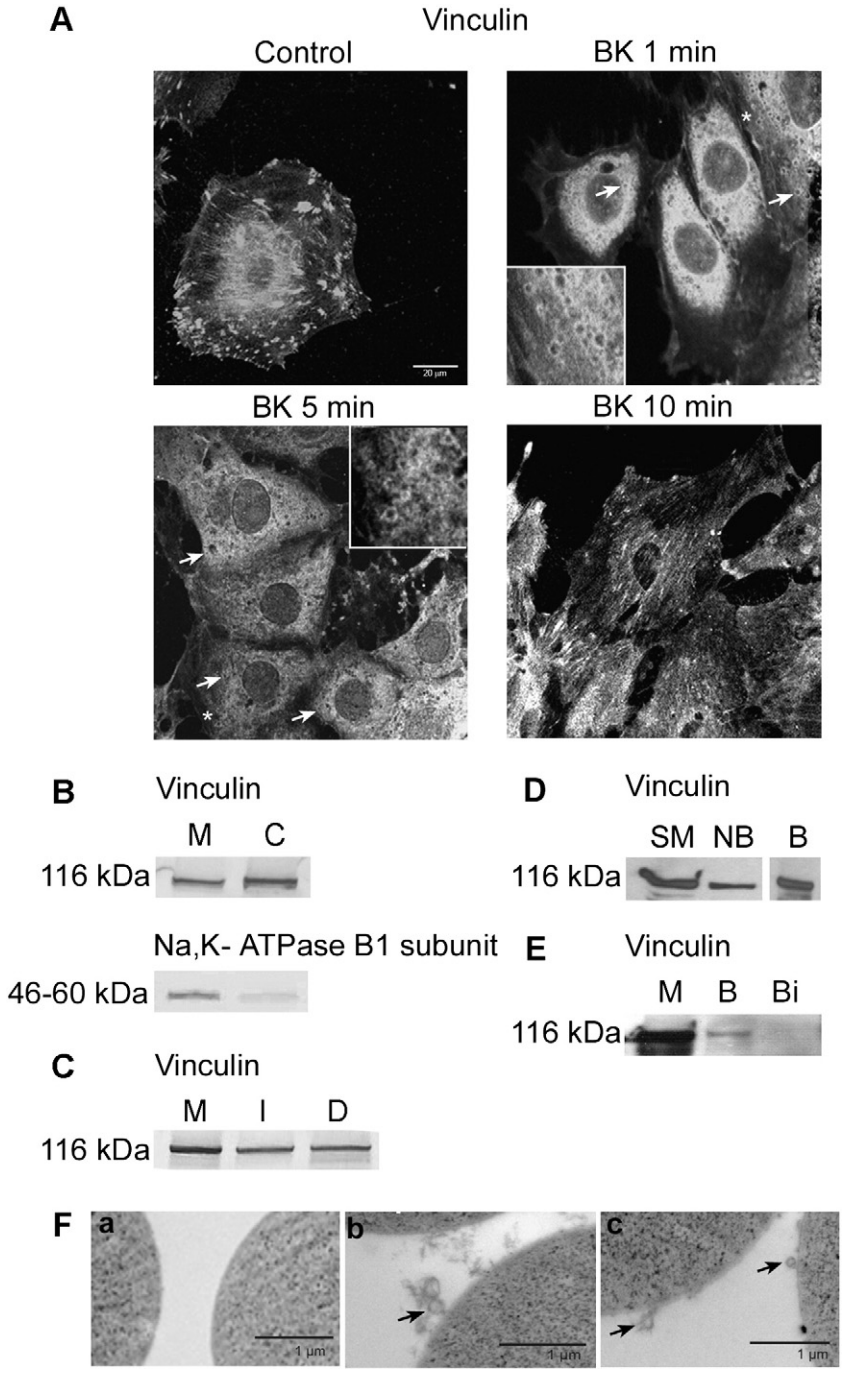

Fig. 1. Isolation of vinculin-containing vesicles from renal papillary collecting duct cells. A) Subconfluent cultured cells were incubated with 1 μM bradykinin (BK) for 1, 5, and 10 min, and immunostained with an antibody against vinculin and analyzed with confocal microscopy. Arrows point to vinculin-positive vesicles. Insets correspond to an enlargement of the region indicated with an asterisk. Representative images of three experiments are shown. Bar, 20 μm. B) Vinculin distribution in cytosol (C), and microsome (M) samples obtained from renal papillary collecting duct cells as described in Materials and methods, and equivalent amounts of protein were resolved by SDS-PAGE and immunoblotted for vinculin and Na,K-ATPase β1 subunit. C) Immunoisolation of vinculin-containing vesicles. About 200 μg of microsomes (M) was used as starting material (input fraction). Immunoisolated vesicles bound to the magnetic beads obtained by applying the direct (D) and the indirect (I) technique were analyzed by SDS-PAGE and immunoblotted for vinculin. D) About 200 μg of postnuclear supernatant was used as starting material (SM). Bound (B) and non-bound (NB) material obtained by applying the direct technique was analyzed by SDS-PAGE and immunoblotted for vinculin. Different parts of the same membrane are shown. E) As a negative control, beads coated with anti-cyclin D monoclonal antibody as irrelevant antibody (Bi) were used. F) Morphological characterization of the immunoisolated vesicles. Samples were prepared for electron microscopy using standard procedures. (a) Shows the control sample in which the primary antibody had been omitted. (b) and (c) represent the bound subfraction in which most of the immunoadsorbed vesicles are small and free of content (arrows). Partial view of sectioned magnetic beads is shown. Bar, 1 μm.

serum albumin) carried in or attached to vesicles, but probably are not part of the trafficking apparatus. Thus, we conclude that vinculin-containing intracellular vesicles are heterogeneous and include rough endoplasmic reticulum.

3.2. Characteristics of vinculin association with vesicle membrane

We further examined the vesicle-membrane association properties of vinculin. Microsomal fractions obtained from renal papillary slices

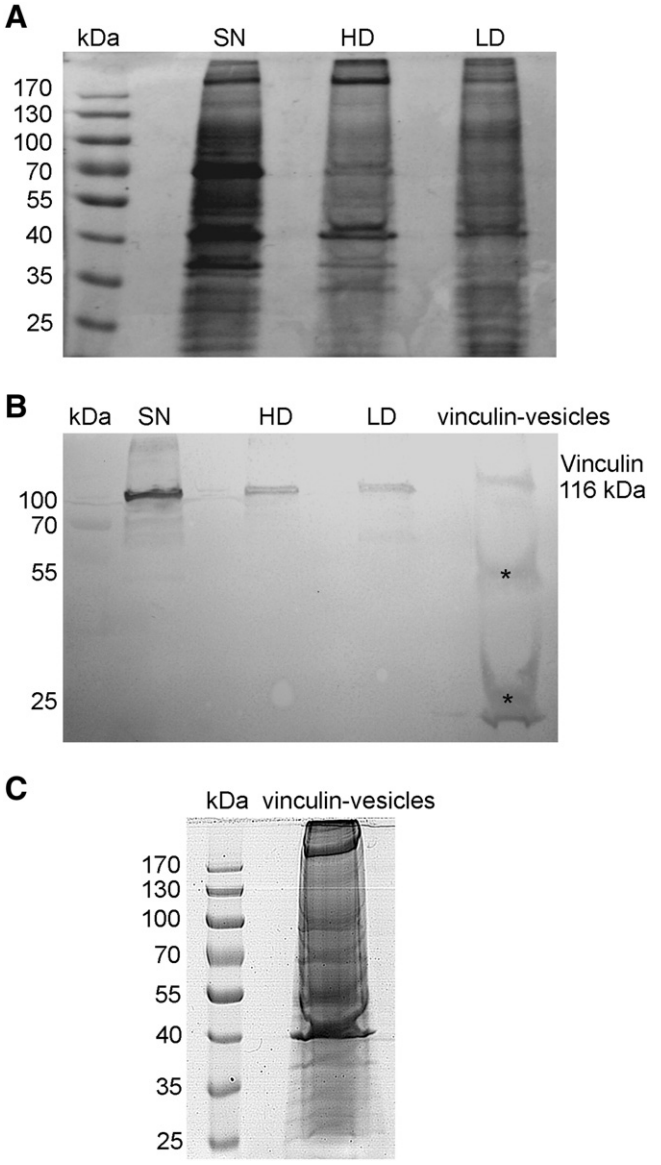

Fig. 2. SDS-polyacrylamide gel electrophoresis and Western blot analyses showing the different fractions obtained during the differential centrifugation. A) Samples of SN (4000 *g* for 10 min centrifugation supernatant), HD (high density membrane fraction), and LD (low density membrane fraction) were obtained as described in Materials and methods, and equal amounts of total protein (50 μg) were developed in a 10% SDS-PAGE and stained with Coomassie blue. B) SN, HD, LD and vinculin-vesicle (50 μl) samples were obtained as described in Materials and methods, and equal amounts of total protein (40 μg) were developed in a 10% SDS-PAGE and analyzed by Western blotting. Vinculin was markedly enriched in SN as compared with HD, LD and vesicles samples. Bands indicated with asterisks correspond to heavy (55 kDa) and light (25 kDa) Ig G chain chains. A representative immunoblot is shown. C) Vinculin-containing vesicles were immunoisolated from LD membranes fraction (1000 μg of protein). Proteins were resolved by SDS-PAGE using 10% polyacrylamide and stained with Coomassie blue. The gel was sliced for in-gel trypsinization and LC–MS/MS analysis.

incubated with BK were extracted with PBS, high-salt (1.0–3.0 M KCl) or high-pH solutions (0.5 and 0.1 M Na_2CO_3 pH 10) and separated into membrane pellets and soluble fraction by ultracentrifugation at 100,000 *g*. When microsomes were subjected to PBS treatment, most of the protein was detected in the 100,000 *g* pellet (Fig. 3A). Thereafter, as vesicles were treated with increasing concentrations of KCl, the amount of vinculin in the supernatant increased, reflecting its release from the membrane vesicles, which is a characteristic of peripheral proteins. With respect to the treatment with Na_2CO_3, a concentration as low as 0.5 M Na_2CO_3 was enough to release vinculin from the particulate fraction, thus denoting high efficiency of the change in pH to dissociate

Table 1
Summary of proteins identified in association with intracellular vinculin vesicles in renal papilla collecting duct cells.

Proteins in decreasing order of molecular weight
Myosin-9
Vinculin
Heat shock protein HSP 90-beta
Heat shock protein HSP 90-alpha
Gelsolin
Alpha-actinin-4
Transitional endoplasmic reticulum ATPase
Calnexin
Serum albumin
Heat shock cognate 71 kDa
Heat shock 70 kDa 1A/1B
ATP synthase subunit alpha, mitochondrial
Tubulin beta-4B chain
Tubulin alpha-1B chain
Ig gamma-1 chain C region
ATP synthase subunit beta, mitochondrial
Tubulin beta-5 chain
Tubulin alpha-1A chain
Actin, cytoplasmic 1
Actin, cytoplasmic 2

vinculin from the membrane (Fig. 3B). Membrane association of vinculin was also demonstrated by cloudy point precipitation with Triton X-114, which is widely used to characterize the association of proteins with the membrane [18]. In such assay, when the cloudy point temperature is reached, Triton X-114 solution separates into a lighter-upper phase of aqueous solution and a detergent-rich lower phase. Integral

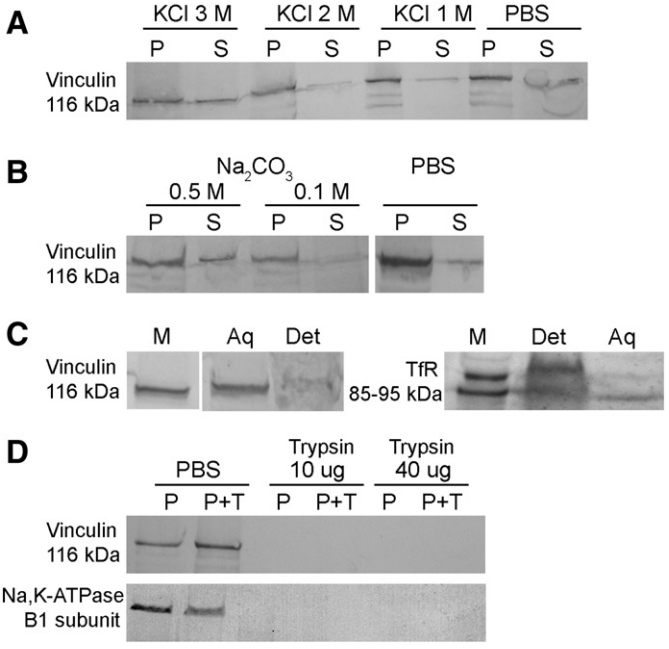

Fig. 3. Characteristics of vinculin association with vesicle membranes. A) High-salt and B) alkaline extraction of microsomal fraction isolated from renal papillary slices treated with BK. The pellets (P) and supernatants (S) were analyzed for vinculin by immunoblot analysis. Different parts from different membranes are shown. C) Triton X-114 extraction of microsomal fraction (M) and phase separation. Equal volumes of the aqueous phase (Aq) and detergent phase (Det) were analyzed for vinculin and for transferrin receptor (TfR). Different parts of the same membrane are shown. D) Membrane orientation of vinculin, as determined by proteolysis. Microsomal fractions were incubated at 0 °C with increasing amounts of trypsin, with or without 1% Triton X-100. Vinculin and the Na,K-ATPase β1 subunit were analyzed by immunoblot. Results correspond to one of three independent experiments.

proteins with amphiphilic nature have to be recovered in the detergent phase, whereas most peripheral proteins are found in the aqueous phase. Here, when microsomes were resuspended in Triton X-114 solution and the phases separated, most of the vinculin from the microsomal membranes was recovered in the aqueous phase, while its presence in the detergent phase was negligible (Fig. 3C), which is characteristic of peripheral membrane proteins. As positive control for integral membrane protein, we used TfR. Most TfR was recovered in the detergent phase (Fig. 3C). To verify the membrane orientation of vinculin, the microsomes were subjected to trypsin digestion in the presence or absence of Triton X-100, and the protease-resistant membrane fractions recovered in pellets were analyzed by immunoblot. No positive signals were detected in the immunoblot of trypsin-treated samples, reflecting that vinculin was highly sensitive to trypsin digestion still in the absence of detergent (Fig. 3D). The Na,K-ATPase β1 subunit, which is a single transmembrane segment whose mass is mostly on the extracellular side of the membrane, was used as control. The monoclonal antibody raised against an epitope located in the external domain of the β1 subunit detected the protein in non-treated membranes but not in samples digested with trypsin in the absence or presence of detergent (Fig. 3D).

Taken together, these results confirm that vinculin is intracellularly carried by vesicles as a peripheral membrane-associated protein, oriented to the cytosol. Because of the high sensitivity to be displaced by high-salt solutions, it seems that the association occurs via electrostatic interactions.

In a second step, we biochemically analyzed the immunoisolated vesicles to determine the presence of proteins involved in vesicle traffic. Taking into account that Rab11 has been proposed to function in transferrin recycling [21] and that Rab5 is localized in early endosomes [20], we investigated whether Rab11 and Rab5 cofractionated with vinculin during immunoisolation. It is well known that phosphoinositides have a role in defining vesicle identity and in recruiting both cytosolic and membrane proteins to specific membranes [21]. It is currently considered that vinculin has to bound to PtdIns(4,5)P_2 to stay in FA plaques [8]. On the other hand, we have reported that in renal papillary collecting duct cells a decreased production of PtdIns(4,5)P_2 compromises the recruitment of vinculin into FAs [13]. Thereafter, by using an antibody against PtdIns(4,5)P_2, we determined the presence of PtdIns(4,5)P_2 associated with vinculin in the immunoisolated vesicles. As negative control, we used beads where vinculin antibody had been omitted. Positive signals for both Rab5 and Rab11, as well as for TfR, were detectable by immunoblot in immunoisolated vesicles (Fig. 4A), thus reflecting that vinculin-positive vesicles are part of the vesicle intracellular traffic of proteins. A band of molecular mass ~116 kDa, compatible with PtdIns(4,5)P_2 bound to vinculin was also detected. No positive signal was present in the negative control.

We have previously found that in renal papillary collecting duct cells, vinculin binds to talin in DRM in the assembled FA complex [13] and that, after BK treatment, while vinculin is released from FAs, talin remains associated with the plasma membrane [14]. Consequently it is expected that talin is not present in the BK-induced-vinculin containing vesicles. Since paxillin is another FA protein that binds with vinculin in FAs [9], we also looked for its presence. As expected, neither talin nor paxillin were detected in vinculin-containing vesicles (Fig. 4B). To perform the immunoblot analysis of talin and paxillin, the volumes of the B and NB fractions were adjusted to contain the same amount of total protein (50 μg). We duplicated the amount of loaded protein to corroborate these results. It is expected that if present, paxillin and talin are diluted and not detectable in the NB fraction, but in the same experimental condition vinculin is clearly detected in the NB fraction (Figs. 1D and 5B). In our knowledge most of the NB vinculin corresponds to the large soluble cytosolic pool. By contrast it has been reported that cytosolic talin and paxillin suffer calpain degradation [22]. For this reason, as a positive control, we loaded a sample of microsomes where talin and paxillin were detected.

The presence of positive signal for TfR, Rab5 and Rab11, together with PtdIns(4,5)P_2-bound vinculin in the immunoisolated vesicles, strongly suggests that the BK-induced internalized vinculin may be recruited to the Rab5-positive endosomal compartment, and to the Rab11-positive recycling endosomes. The absence of both talin and paxillin suggests that traffic is selective for the released vinculin but not for the entire FA complex.

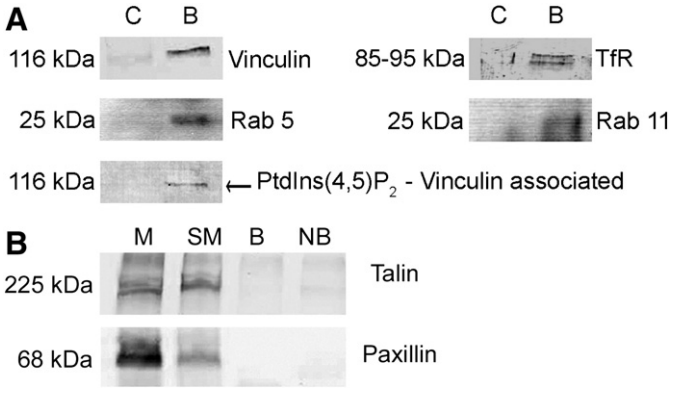

Fig. 4. Biochemical analysis of immunoisolated vesicles. A) Immunoisolated vesicles bound to the beads (B) were analyzed by SDS-PAGE and immunoblot with the use of specific antibodies against the indicated proteins. As a negative control, we used beads where vinculin antibody had been omitted (C). B) About 200 μg of postnuclear supernatant was used as starting material (SM). Bound (B) and non-bound (NB) material was analyzed by SDS-PAGE and immunoblot for talin and paxillin. A sample of microsomes (M) was also resolved to show the presence of both proteins. Results correspond to one of three independent experiments.

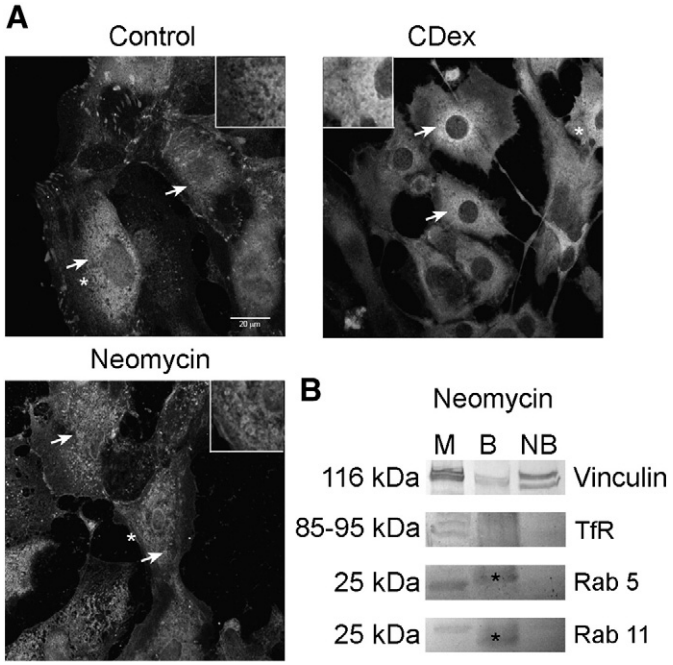

Fig. 5. Vinculin-containing vesicles are present in cells treated with neomycin and methyl-β-cyclodextrin. A) Subconfluent cultured cells were incubated with 1 mM neomycin for 10 min or 5 mM methyl-β-cyclodextrin (Cdex) for 30 min, and immunostained with an antibody against vinculin and analyzed with confocal microscopy. Arrows point to vinculin-positive vesicles. Insets correspond to enlargement regions indicated with an asterisk. Representative images of three independent experiments are shown. Bar, 20 μm. B) Immunoisolation of vinculin-containing vesicles from neomycin-treated tissue. About 200 μg of postnuclear supernatant was used as starting material. Bound (B) and non-bound (NB) material was analyzed by SDS-PAGE and immunoblotted for the indicated protein. A sample of microsomes (M) was also resolved to show the presence of both proteins. The asterisks correspond to the IgG light chain (~23–26 kDa). Results correspond to one of three independent experiments.

3.3. The alteration in lipid membrane composition evokes the formation of non-recycling vinculin-containing vesicles

In renal papillary collecting duct cells, FAs are part of a DRM [13]. To investigate whether the formation of vinculin-containing vesicles is a BK-specific or a general phenomenon, we treated cultured renal papillary collecting duct cells with the lipid membrane-affecting agents methyl-β-cyclodextrin (CDex) and neomycin. Neomycin is a known PtdIns(4,5)P_2-sequestering agent and CDex is a cholesterol-depleting agent. We have previously shown that both agents induce an overall change in the DRM phospholipid profile and dissipation of vinculin- and talin-immunostained FAs with no further reconstitution [13]. After neomycin and CDex treatment of cultures of renal papillary collecting duct cells, we observed the formation of vesicle-like structures containing vinculin in the cytosol (Fig. 5A, arrows and insets). To find out whether these vesicles exhibited biochemical characteristics similar to those isolated from BK-treated tissue, we immunoisolated them from the postnuclear supernatant of renal papillary slices treated with neomycin and CDex. Although we duplicated the amount of protein loading to perform immunoblot analysis, we found no markers of the recycling endosomal compartment, such as Rab5, Rab11 or TfR, in the immunoisolated vesicles from neomycin treated tissue (Fig. 5B). We interpret that the vinculin associated to vesicle-like structures (arrows) recovered in the B fraction (Fig. 5B), corresponds to a smaller pool of vinculin membrane — associated if compared with the large cytosolic pool. TfR, Rab5 and Rab11 did not appear in B because they are not part of such vesicles and did not appear as NB because they are at very low concentration in the cell, and due to the fact that experimental protocol is diluted (NB volume ~ 1 ml) and not detectable. For this reason, like with talin and paxillin, as a positive control we loaded a sample of microsomes, where the protein signals were detected. Similar results were obtained with CDex (not shown). Thus, these intracellular structures may correspond to a plasma membrane vesiculation but not to a physiological endosomal formation. Interestingly, we observed vesicle-like structures containing vinculin in the cytosol of untreated cells (Fig. 5A, arrows and insets). Our results suggest that the formation of vesicles containing vinculin that also carry the markers of the recycling endosomal compartment is not a general phenomenon. Their formation could be a physiological mechanism to reuse the internalized vinculin to reassembly new FAs, which occurs after long time of BK stimulation. We have previously reported that FAs that reassemble occur after BK stimulation but not after neomycin or cyclodextrin treatment [13,14]. We used the term physiological because this phenomenon is observed when the system is activated by the physiological hormone BK, but it was not observed when nonphysiological agents such as neomycin or cyclodextrin were used.

3.4. The expression of Rab5 and Rab11 in vinculin-containing vesicles depends on the time of BK stimulation

We have previously shown that BK induces the perinuclear accumulation of vinculin at 1 min, that it diffuses in the cytosol after 5 min, and that it then reaches the periphery of the cell at 10 min [15]. To follow the dynamics of vinculin-containing vesicle formation, we treated cultured renal papillary collecting duct cells with BK for 1, 5 and 10 min and examined the colocalization of vinculin with Rab5 (a marker of early endosomes) and Rab11 (which mediates recycling of endocytic vesicles) [23]. To this end, we used confocal microscopy and quantitative analysis of the extent of colocalization by calculating Manders' Overlap Coefficient (MOC) in the marginal and perinuclear cell regions. The Manders' Overlap Coefficient (MOC) was used to estimate the degree of colocalization [20]. Its value is defined from 0 to 1, and a MOC $\geq$ 0.7 indicates colocalization. For the quantitative analysis, we selected confocal horizontal optical cross sections at middle cell plane from the basal side, where most of the vesicles are located. Vinculin–Rab5 colocalization analysis demonstrated a high degree of colocalization in the marginal and perinuclear cell regions, even in controls (Fig. 6). Vinculin also colocalized with Rab11 in the perinuclear region in both untreated and BK-treated cells. In the marginal region, overlapping was observed only after 5 and 10 min of BK treatment (Fig. 7).

Our next step was to determine the contribution of vinculin and Rab5/Rab11 to the area of colocalization in untreated and BK-treated cells, by calculating the overlap coefficients K1 and K2, corresponding to vinculin (K1, red channel) and to Rab5 or Rab11 (K2, green channel) (Fig. 8). The analysis of these coefficients showed a different contribution of both molecules depending on the time of stimulation and the cell region analyzed. The marginal region of untreated cells showed maximal contribution of Rab5 and minimal contribution of vinculin, suggesting that the presence of Rab5-positive vesicles is almost empty of vinculin under non-stimulated conditions. After BK stimulation, the degree of vinculin contribution gradually increased, while Rab5 contribution decreased, denoting vinculin enrichment in Rab5-positive vesicles (Fig. 8A). In the perinuclear region of untreated cells, the contribution of both vinculin and Rab5 was quite similar, which indicates that under non-stimulated conditions there exist Rab5-positive vesicles containing vinculin in the marginal region of the cell. After 1 min of BK stimulation, vinculin contribution increased, denoting vinculin enrichment. After 5 min, Rab5 contribution also increased, decreasing thereafter (Fig. 8B).

With regard to vesicles containing Rab11, in both cell regions of untreated cells, the contribution of vinculin was very low but increased gradually after 1 and 5 min of BK stimulation, denoting vinculin enrichment, and then decreased thereafter (Fig. 8C and D).

We also evaluated whether BK causes changes in the amount of Rab5 and Rab11 present in the vesicles isolated from renal papillary slices either untreated or treated with BK for 1, 5 and 10 min. Equal amounts of total proteins of each experimental condition were developed in SDS-PAGE and analyzed by immunoblot. After BK stimulation, the amount of vesicular Rab5 decreased when compared with that present in vesicles isolated from untreated tissue (C vs BK 1 min, vs BK 5 min, and vs BK 10 min, $p < 0.05$) (Fig. 9A). By contrast, the amount of Rab11 significantly increased after 10 min of BK treatment (C vs BK 10 min, $p < 0.05$) (Fig. 9B). In addition, the amount of vinculin present in the isolated vesicles gradually increased with time after BK treatment (C vs BK 1 min, vs BK 5 min, and vs BK 10 min, $p < 0.05$) (Fig. 9C). Due to the experimental protocol design, these results represent the total amount of these proteins present in the whole sample of vesicles isolated from renal papillary slices without discrimination between marginal and perinuclear vesicles.

Taken together, these results suggest that in untreated cells, Rab5- and/or Rab11-positive vesicles are present in the cytosol, but are not overloaded with vinculin. After BK stimulation, vinculin seems to be recruited to the vesicle-like structures containing Rab5 and/or Rab11. The quantitative analysis of the immunoblot showed different amounts of Rab5 and Rab11 in vinculin-containing vesicles. The modification of the contribution to the colocalization of vinculin and Rab5/Rab11 reflects changes in the level of Rabs in the vesicles to ensure the transportation of the vinculin that is not forming FAs, namely the cytosolic pool.

4. Discussion

It is accepted that, in every cell type, vinculin exists in a cytosolic and in a cytoskeletal pool, considering as the cytoskeletal pool the vinculin that is part of the FAs and/or adherent junction complexes and as the cytosolic pool the one formed by an auto-inhibited soluble conformation of the protein [5]. It has been reported that in cultured chick embryo fibroblasts, vinculin's half-life is 2–3 times shorter in the cytoskeletal pool than in the cytosolic pool, which suggests that the incorporation of cytosolic vinculin into the cytoskeleton does not involve a simple equilibrium between the two pools [4]. This is the first time that vinculin is found localized in vesicles, a finding that challenges the

prevailing model of vinculin distribution in the cytosol. In the present work, we show that the cytosolic pool is composed of both the vinculin associated with the vesicle membranes, corresponding to the magnetic bead-"bound fraction", and of the vinculin present in the cytosol in a soluble form, which corresponds to the magnetic bead-"unbound fraction". Taking advantage of the fact that BK stimulation of collecting duct cells induces vinculin internalization [15], we decided to explore the formation of vinculin-containing vesicles and characterize them biochemically. We isolated the vesicles by using the direct technique of the immunomagnetic method. The morphological analysis of the immunoisolated fraction showed that it consists of small empty vesicles.

Vinculin is not a transmembrane protein and it would be expected that it associates with intracellular vesicles peripherically. To corroborate the nature of vesicle association properties of vinculin, alkaline and high-salt extraction, Triton X-114 phase separation and protease protection assay of the microsomal fractions were performed. As expected, our results demonstrated that vinculin is peripherically associated with the vesicles, and oriented to the cytosol and probably associated with the membranes via electrostatic interactions.

We also showed that these vinculin-positive vesicles contain not only proteins reported to coordinate vesicle traffic, namely Rab11 and Rab5, but also TfR. Rab GTPases are specifically associated with different organelles within the cell [23]. Rab5 is present in early endosomes [24] and two distinguishable populations of early endosomes have been described, the dynamic and the static populations. The dynamic group matures rapidly into late endosomes, which later proceed towards the degradation pathway involving lysosomes. Taking into account that we have previously demonstrated that BK induces an intracellular redistribution of vinculin with no changes in its total amount [14], we suggest that the internalized vinculin could be entering the Rab5-positive static one, whose maturation is slower [25], thus justifying the value of the MOC obtained. Moreover, the fact that in the marginal region of untreated cells, Rab5 contribution to colocalization was higher than that of vinculin, and that after BK stimulation the degree of vinculin contribution gradually increased as denoted by the analysis of the overlap coefficients K1 (vinculin) and K2 (Rab5), we suggest that, at first, the BK-induced internalized vinculin enters the pre-existing Rab5-positive static early endosomal compartment. On the other hand, it is accepted that Rab11 is a GTPase marker within the recycling compartment [23], and since after internalization, TfR is trafficked through early and recycling endosomes [26], both molecules are used as tools to visualize these compartments. In untreated cells and cells treated with BK for 1 min, vinculin did not colocalize with Rab11 in the marginal region, but did so after longer times of BK stimulation. These results denote that in non-stimulated conditions, marginal recycling endosomes are free of vinculin, but as BK stimulation occurs, vinculin enters such compartment probably as a way to further reach the plasma membrane. In the perinuclear region, in both untreated and BK-treated cells, vinculin colocalizes with Rab11, showing stronger overlap after 5 and 10 min, reflecting that, in basal conditions, there exists a smaller pool of vesicles that contain vinculin that probably comes from the basal turnover of the protein associated with FAs or adherent junctions. After BK stimulation, it appears that such a pool of early endosomes containing vinculin increases as a consequence of its dissipation from the cytoskeletal pool. So, after BK stimulation, once in the early endosomes, vinculin may be sorted to the recycling pathway. This interpretation is supported by the fact that in both cell regions of untreated cells the contribution of vinculin in the process of colocalization is very low, and increases after

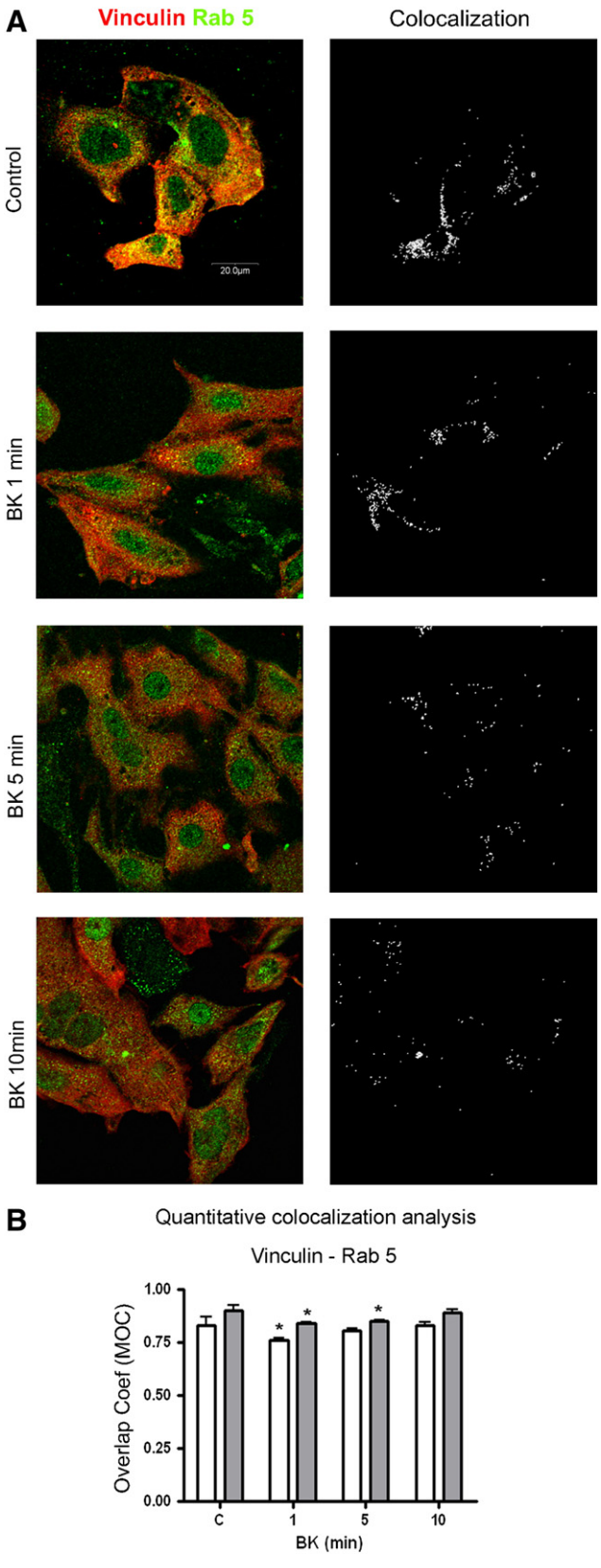

Fig. 6. BK induces the formation of vesicle-like structures containing vinculin which colocalize with Rab5 in renal papillary collecting duct cells. A) Subconfluent cultured cells were stimulated with 1 μM BK for 1, 5 and 10 min. After fixation, cells were simultaneously immunostained with antibodies against vinculin (red) and Rab5 (green). The double color merges of single confocal planes are shown to indicate the extent of colocalization between vinculin and Rab5. The colocalization study was performed using the Image Pro colocalization module. Representative images of three experiments are shown. Scale bar: 20 μm. (B) An average of the Manders' Overlap Coefficient (MOC) to estimate the degree of colocalization between vinculin and Rab5 in the perinuclear (gray bars) and marginal (white bars) regions for each time point of BK stimulation is shown. A value equal to or higher than 0.7 implies colocalization. Values are means ± standard error (n = 3). *Significantly different from control, $p < 0.05$.

BK stimulation, as assessed by the analysis of the overlap coefficients K1 (vinculin) and K2 (Rab11). The increase in the total amount of vinculin and Rab11 and the decrease in Rab5 in the vinculin-containing vesicles after BK treatment observed in the immunoblot analysis are in agreement with this interpretation. This is also consistent with our previous report where we showed the appearance of a high density of vinculin fluorescence concentrated in the perinuclear region, where the recycling compartment is located [15].

Although our LC–MS/MS analysis did not identify TfR as a component in vinculin vesicles, its presence was demonstrated by immunoblotting. However, we identified alpha-actinin, which is a subunit of the protein complex CART (cytoskeleton-associated recycling or transport), that is necessary for efficient TfR recycling [27]. It is known that a negative result using mass spectroscopy does not necessarily imply the absence of a particular protein. Moreover, we also identified myosin-9, which appears to play a role during cell spreading, and plays an important role in cytoskeleton reorganization, focal contacts formation, and lamellipodial retraction [28]. Although it appears clear that intracellular vinculin is present in recycling endosomes, our LC–MS/MS analysis of immunoisolated vinculin vesicles from the renal papillae collecting duct cells also revealed endoplasmic reticulum-resident proteins. This result demonstrates that in addition to recycling endosomes, intracellular vinculin vesicles also include the rough endoplasmic reticulum. Obviously vinculin and other cell membrane proteins are translated at the rough endoplasmic reticulum, and the presence of vinculin in rough endoplasmic reticulum membranes implies that new vinculin that is being produced has a sufficient residence time in the rough endoplasmic reticulum to manifest itself in this analysis. The transitional endoplasmic reticulum ATPase identified in the LC–MS/MS analysis is involved in the formation of the transitional endoplasmic reticulum [29]. The transfer of membranes from the endoplasmic reticulum to the Golgi apparatus – which is an ATP-dependent process – occurs via 50–70 nm transition vesicles which derive from part-rough, part-smooth transitional elements of the endoplasmic reticulum [29]. Probably these vesicles transport vinculin in the biosynthetic route, and with no doubt due to its small size sediments in the LD membrane fraction. We propose a model where the vinculin present in the cytosolic pool moves between the free cytosolic form and the vesicle-associated form, to be further included in the FA complexes. Another potential route of vinculin trafficking from the intracellular compartment to the plasma membrane could be via recycling endosomes. Vinculin can hypothetically move from the TGN directly into recycling endosomes. An additional possibility is that vinculin can be translocated directly from the TGN to plasma membrane via secretory vesicles but we have no experimental evidence to support this hypothesis.

Our results strongly suggest that vinculin-containing vesicles are heterogeneous and travel through the recycling pathway to sites of plasma membrane of renal collecting duct cells, where vinculin-immunostained FAs reassemble after a long period (10 min) of BK stimulation.

It is known that PtdIns(4,5)P_2 is a primary regulator of proteins involved in the recycling of cargoes back to the plasma membrane [30–32]. In addition, we have previously reported failure in vinculin internalization in cells treated with LiCl, a phosphoinositide synthesis inhibitor [15]. In the present report, we showed that PtdIns(4,5)P_2 is present in our isolated vinculin-containing vesicles. Because of the high affinity of PtdIns(4,5)P_2 to bind vinculin, we can hypothesize that the decreased production of PtdIns(4,5)P_2 could compromise the

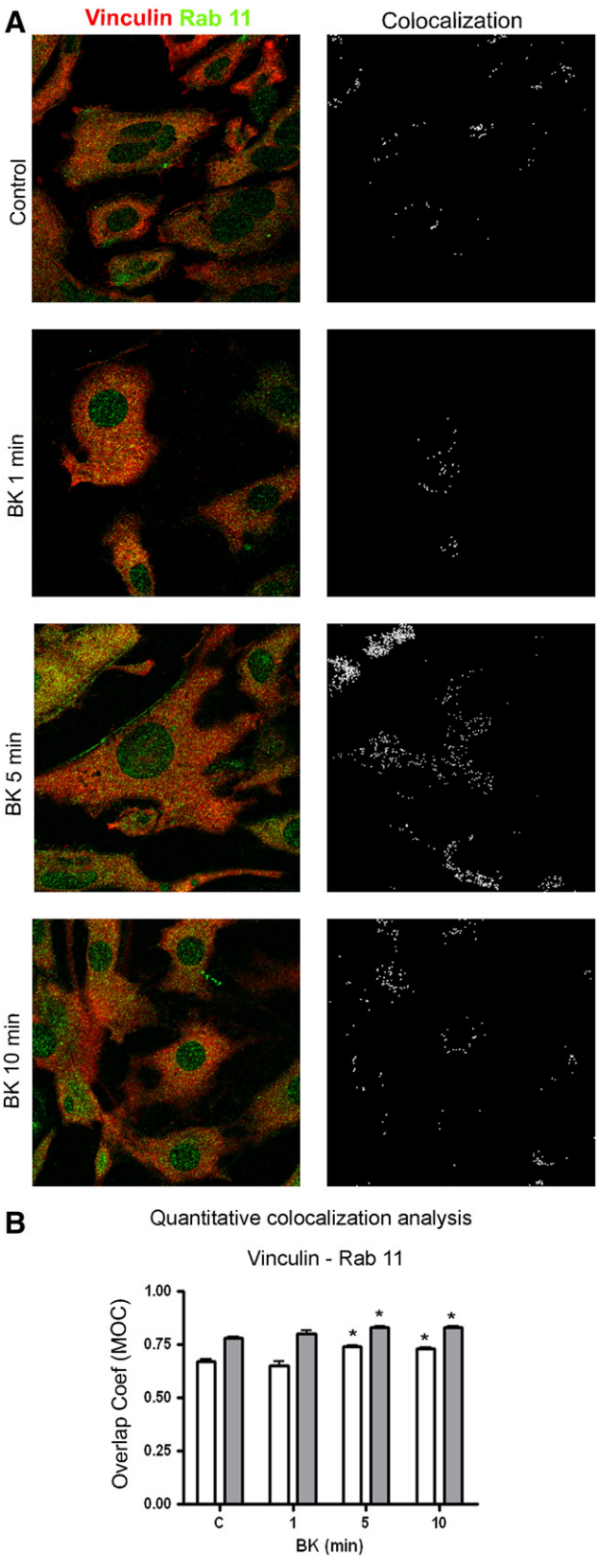

Fig. 7. BK induces the formation of vesicle-like structures containing vinculin which colocalize with Rab11 in renal papillary collecting duct cells. A) Subconfluent cultured cells were stimulated with 1 μM BK for 1, 5 and 10 min. After fixation, cells were simultaneously immunostained with antibodies against vinculin (red) and Rab11 (green). The double color merges of single confocal planes are shown to indicate the extent of colocalization between vinculin and Rab11. The colocalization study was performed using the Image Pro colocalization module. Representative images of three experiments are shown. Scale bar: 20 μm. (B) An average of the Manders' Overlap Coefficient (MOC) to estimate the degree of colocalization between vinculin and Rab11 in the perinuclear (gray bars) and marginal (white bars) regions for each time point of BK stimulation is shown. A value equal to or higher than 0.7 implies colocalization. Values are means ± standard error ($n = 3$). *Significantly different from control, $p < 0.05$.

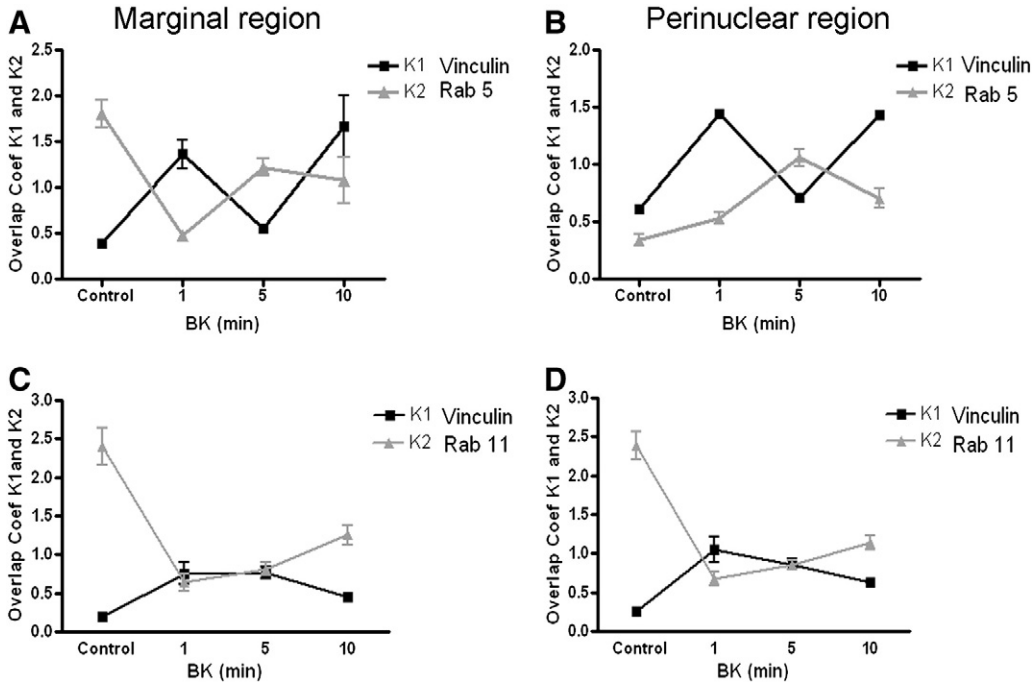

Fig. 8. Quantitative colocalization analysis between vinculin and Rab5/Rab11 in the perinuclear and marginal regions of renal papillary collecting duct cells. An average of the overlap coefficients K1 (vinculin) and K2 (Rab5 or Rab11) in the marginal region (A and C) and in the perinuclear region (B and D) of the cell is shown for each time point of BK stimulation. Values are means ± standard error (n = 3).

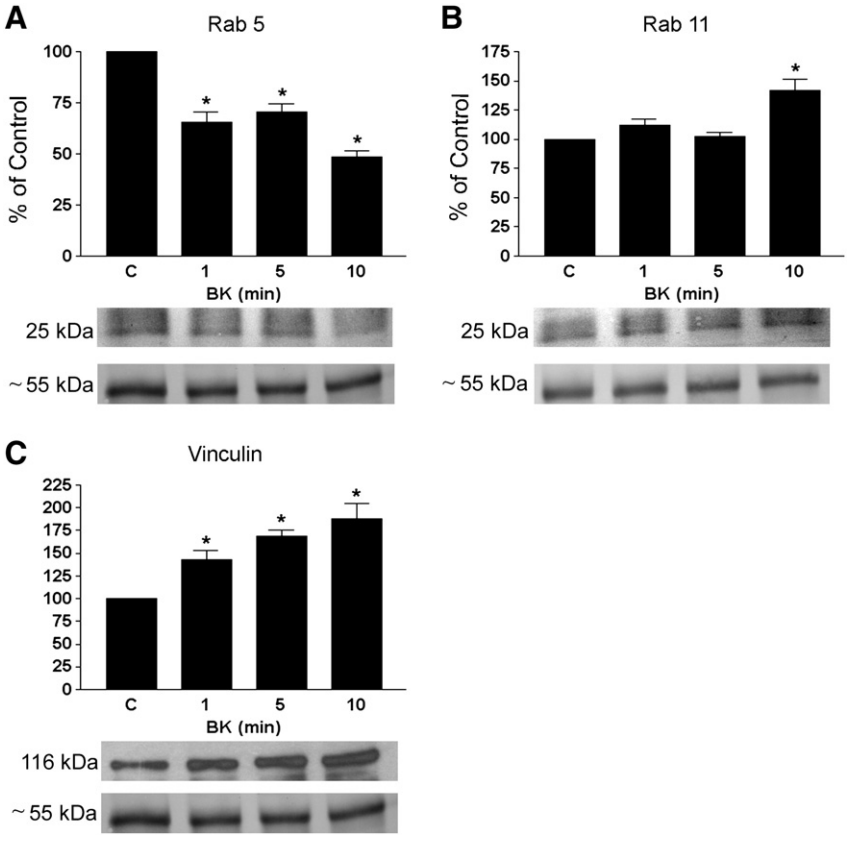

Fig. 9. Western blot analysis for Rab5 and Rab11 levels in vinculin-containing vesicles. Vinculin-containing vesicles were immunoisolated from renal papillary slices either untreated or treated with BK for 1, 5 and 10 min. Equal amounts of total proteins of each experimental condition were developed in SDS-PAGE and analyzed by immunoblot with the use of specific antibodies against the indicated proteins. Vinculin was evidenced by using the ECL kit, and the same membrane was stripped and reprobed for Rab5. Rab11 and Rab5 were evidenced by using avidin–biotin–peroxidase and 3,3′diaminobenzidine. Protein loading was controlled by staining with Coomassie blue. For loading control, the lines corresponding to the IgG heavy chain (~55 kDa) are shown. Values are means ± standard error of three experiments. Representative immunoblots are shown. *Significantly different from control, $p < 0.05$.

recruitment of vinculin to the vesicle membranes. On the other hand, it is known that Rab5 participates in PtdIns(4,5)P_2 turnover by the recruitment of a class I PI3-kinase (PI3K) [33] or a PI phosphatase [34]. So, the presence of Rab5 in these vesicles could be controlling vinculin recruitment and delivery to newly forming FAs by defining the presence or absence of PtdIns(4,5)P_2 in restricted vesicle membrane domains.

We also observed the presence of vesicle-like structures containing vinculin in the cytosol of renal papillary collecting duct cells treated with the membrane-affecting agents neomycin and methyl-β-cyclodextrin, which, like BK, cause dissipation of vinculin-stained FAs [13]. Such vinculin-containing vesicles contained neither TfR nor Rab5/Rab11, which led us to consider that such structures do not correspond to the physiological endosome recycling pathway but came more probably from the plasma membrane vesiculation that occurs as a consequence of alterations in the membrane lipid raft, as we have previously reported [13]. This consideration is consistent with the fact that after treatment with the membrane affecting agents, FAs disrupt and did not reassemble further.

A study performed in living cells reported that cytosolic vinculin is inactive (closed conformation) at least with respect to its actin-binding potential, and when is being recruited to focal adhesions, the vinculin remains in the nonactin binding conformation, and a second signal or event must be required to link vinculin to actin [35]. Moreover, pulse-chase experiments demonstrated that pre-existing soluble vinculin (and talin) in the cytosolic pool could be utilized when cells reformed their cytoskeleton after trypsin treatment, and only a small portion of newly synthesized vinculin for constructing (or maintaining) the cytoskeletal pool is used [4]. Taken into account these considerations, it is possible that our nonbound fraction could be containing the inactive cytosolic soluble pool of vinculin reported by Lee and Otto [4]. With regards the origin, the nonbound fraction probably contains the large pre-existing cytosolic pool, the newly synthesized, and in a smaller proportion the membrane-bound vinculin present in the microsomes.

In conclusion, we demonstrate the existence of a third pool of vinculin (the vesicular one) which can serve as an intermediate pool for the reassembly into FAs. We propose a model where the vinculin present in the cytosolic pool moves between the free cytosolic form and the vesicle-associated form, to be further included in the FA complexes. This could be a physiological mechanism through which renal papillary collecting duct cells can reuse the internalized vinculin during FA physiological restructuring. Considering that assembly, disassembly and reassembly of FAs are relevant mechanisms used by cells as a strategy for migration as well as for the establishment of new colonies as part of the process of development and cancer, and that vinculin is a key molecule for the formation of adhesion structures, our finding of the existence of the vesicular pool of vinculin can constitute a relevant physiological mechanism to assume the availability of vinculin and a way to evade its degradation.

5. Conclusions

By using an immunomagnetic method, we isolated vinculin-containing vesicles induced by BK stimulation from collecting duct cells. By analyzing the presence of proteins involved in vesicle traffic, we suggest that vinculin can be delivered in the site of FA reassembly by a vesicular endocytic recycling pathway. Our results demonstrate, for the first time, that besides the cytosolic and cytoskeletal pools of vinculin, there is an additional vesicle-associated pool, which may represent an alternative to the classical model that states that when vinculin is not part of FAs, it remains in the cytosol only in a soluble auto-inhibited conformation. We propose that, when physiologically mobilized, vinculin can enter the endocytic recycling pathway, which could represent a physiological mechanism to reuse the internalized vinculin to reassembly new FAs.

Acknowledgements

We thank Mr Roberto Fernández for confocal microscope technical assistance and Dr Ricardo E Fretes for the electron microscopy study (National University of Cordoba 00-07959/2008).

This work was supported by the National Council for Scientific and Technologic Research-CONICET (PIP-0233), by the National Agency for Scientific and Technologic Promotion (PICT-1038), by University of Buenos Aires and by the National University of La Rioja (8043/09 and 1024/12).

References

[1] B. Geiger, A 130 K protein from chicken gizzard: its localization at the termini of microfilament in cultured chicken cells, Cell 18 (1979) 193–205.
[2] J.J. Otto, Vinculin, Cell Motil. Cytoskeleton 16 (1990) 1–6.
[3] D.R. Critchley, Focal adhesions: the cytoskeletal connection, Curr. Opin. Cell Biol. 12 (2000) 133–139.
[4] S. Lee, J.J. Otto, Vinculin and talin: kinetics of entry and exit from the cytoskeletal pool, Cell Motil. Cytoskeleton 36 (1997) 101–111.
[5] R.P. Johnson, S.W. Craig, An intramolecular association between the head and tail domains of vinculin modulates talin binding, J. Biol. Chem. 269 (1994) 12611–12619.
[6] R.P. Johnson, S.W. Craig, F-actin binding site masked by the intramolecular association of vinculin head and tail domains, Nature 373 (1995) 261–264.
[7] R.P. Johnson, S.W. Craig, The carboxy-terminal tail domain of vinculin contains a cryptic binding site for acidic phospholipids, Biochem. Biophys. Res. Commun. 210 (1995) 159–164.
[8] A.P. Gilmore, K. Burridge, Regulation of vinculin binding to talin and actin by phosphatidylinositol-4-5-bisphosphate, Nature 381 (1996) 531–535.
[9] E. Zamir, B. Geiger, Molecular complexity and dynamics of cell-matrix adhesions, J. Cell Sci. 114 (2001) 3583–3590.
[10] C. Bakolista, D.M. Cohen, L.A. Bankston, A.A. Bobkov, G.W. Cadwell, L. Jennings, D.V. Critchey, S.W. Craig, R. Liddington, Structural basis for vinculin activation at sites of cell adhesion, Nature 430 (2004) 583–586.
[11] P.R.J. Bois, B.P. O'Hara, D. Nietlispach, J. Kirkpatrick, T. Izard, The vinculin binding sites of talin and α-actinin are sufficient to activate vinculin, J. Biol. Chem. 181 (2006) 7228–7236.
[12] T. Laux, K. Fukami, M. Thelen, T. Golub, D. Frey, P. Caroni, GAP43, MARCKS, and CAP23 modulates PI(4,5)2 at plasmalemmal rafts, and regulate cell cortex actin dynamics through a common mechanism, J. Cell Biol. 149 (2000) 1455–1471.
[13] M.G. Márquez, M.C. Fernández-Tomé, N.O. Favale, L.G. Pescio, N.B. Sterin-Speziale, Membrane lipid composition plays a central role in te maintenance of epithelial cell adhesion to the extracellular matrix, Lipids 43 (2008) 343–352.
[14] M.G. Márquez, M.C. Fernández-Tomé, N.O. Favale, L.G. Pescio, N.B. Sterin-Speziale, Bradykinin modulates focal adhesions and induces stress fiber remodelling in renal papillary collecting duct cells, Am. J. Physiol. Ren. Physiol. 294 (2008) F603–F613.
[15] M.G. Márquez, M.C. Fernández-Tomé, N.O. Favale, L.G. Pescio, N.B. Sterin-Speziale, Bradykinin induces the formation of vesicle-like structures containing vinculin and PtdIns(4,5)P_2 in renal papillary collecting duct cells, Am. J. Physiol. Ren. Physiol. 297 (2009) F1181–F1191.
[16] D. Marples, M.A. Knepper, E.I. Christensen, S. Nielsen, Redistribution of aquaporin-2 water channels induced by vasopressin in rat kidney inner medullary collecting duct, Am. J. Physiol. 269 (1995) C655–C664.
[17] C.A. Ecelbarger, J. Terris, G. Frindt, M. Echevarria, D. Marples, S. Nielsen, M.A. Knepper, Aquaporin-3 water channel localization and regulation in rat kidney, Am. J. Physiol. 269 (1995) F663–F672.
[18] C. Bordier, Phase separation of integral membrane proteins in Triton X-114 solution, J. Biol. Chem. 256 (1981) 1604–1607.
[19] J.B. Stokes, C. Grupp, R.K.H. Kinne, Purification of rat papillary collecting duct cells: functional and metabolic assessment, Am. J. Physiol. 253 (1987) F251–F262.
[20] E.M.M. Manders, F.J. Verbeek, J.A. Aten, Measurements of colocalization of objects in dual-colour confocal images, J. Microsc. 169 (1993) 375–382.
[21] E. Daro, P. Van der Sluijs, T. Galli, I. Mellman, Rab 4 and cellubrevin define different early endosomes populations on the pathway of transferring receptor recycling, Proc. Natl. Acad. Sci. U. S. A. 93 (1996) 9559–9564.
[22] S.M. Schoenwaelder, Y. Yuan, P. Cooray, H.H. Salem, S.P. Jackson, Calpain cleavage of focal adhesion proteins regulates the cytoskeletal attachment of integrin αIIbβ3 (platelet glycoprotein IIb/IIIa) and the cellular retraction of fibrin clots, J. Biol. Chem. 272 (1997) 1694–1702.
[23] H. Stenmark, Rab GTPases as coordinators of vesicles traffic, Nat. Rev. Mol. Cell Biol. 8 (2009) 513–525.
[24] J. Rink, E. Ghigo, Y. Kalaidzidis, M. Zerial, Rab conversion as a mechanism of progression from early to late endosomes, Cell 122 (2005) 735–749.
[25] M. Lakadamyali, M.J. Rust, X. Zhuang, Ligands for clathrin-mediated endocytosis are differentially sorted into distinct populations of early endosomes, Cell 124 (2006) 997–1009.
[26] K.M. Mayle, A.M. Le, D.T. Kamei, The intracellular trafficking pathway of transferrin, Biochem. Biophys. Acta 1820 (2012) 264–281.
[27] Q. Yan, W. Sun, P. Kujala, Y. Lotfi, T.A. Vida, A.J. Bean, CART: an Hrs/actinin-4/BERP/myosin V protein complex required for efficient receptor recycling, Mol. Biol. Cell 16 (2005) 2470–2482.

[28] V. Betapudi, Myosin II motor proteins with different functions determine the fate of lamellipodia extension during cell spreading, PLoS One 5 (1) (2010) e8560.
[29] L. Zhang, C.L. Ashendel, G.W. Becker, D.J. Morré, Isolation and characterization of the principal ATPase associated with transitional endoplasmic reticulum of rat liver, J. Cell Biol. 127 (1994) 1871–1883.
[30] N. Abe, T. Inoue, T. Galvez, L. Klein, T. Meyer, Dissecting the role of PtdIns(4,5)P_2 in endocytosis and recycling of the transferrin receptor, J. Cell Sci. 121 (2008) 1488–1494.
[31] O. Cremona, P. De Camilli, Phosphoinositides in membrane traffic at the synapse, J. Cell Sci. 114 (2001) 1041–1051.
[32] G. Di Paolo, P. De Camilli, Phosphoinositides in cell regulation and membrane dynamics, Nature 443 (2006) 651–657.
[33] S. Christoforidis, M. Miaczynska, K. Ashman, M. Wilm, L. Zhao, S.C. Yip, M.D. Waterfield, J.M. Backer, M. Zerial, Phosphatidylinositol-3-OH kinases are Rab5 effectors, Nat. Cell Biol. 1 (1999) 249–252.
[34] H.M. Shin, M. Hayashi, S. Christoforidis, S. Lacas-Gervais, S. Hoepfner, M.R. Wenk, J. Modregger, S. Uttenweiler-Joseph, M. Wilm, M.A. Nystuen, W.N. Frankel, M. Solimena, P. De Camilli, M. Zerial, An enzymatic cascade of Rab 5 effectors regulates phosphoinositides turnover in the endocytic pathway, J. Cell Biol. 170 (2005) 607–618.
[35] H. Chen, D.M. Cohen, D.M. Choudhury, N. Kioka, S.W. Craig, Spatial distribution and functional significance of activated vinculin in living cells, J. Cell Biol. 169 (2005) 459–470.